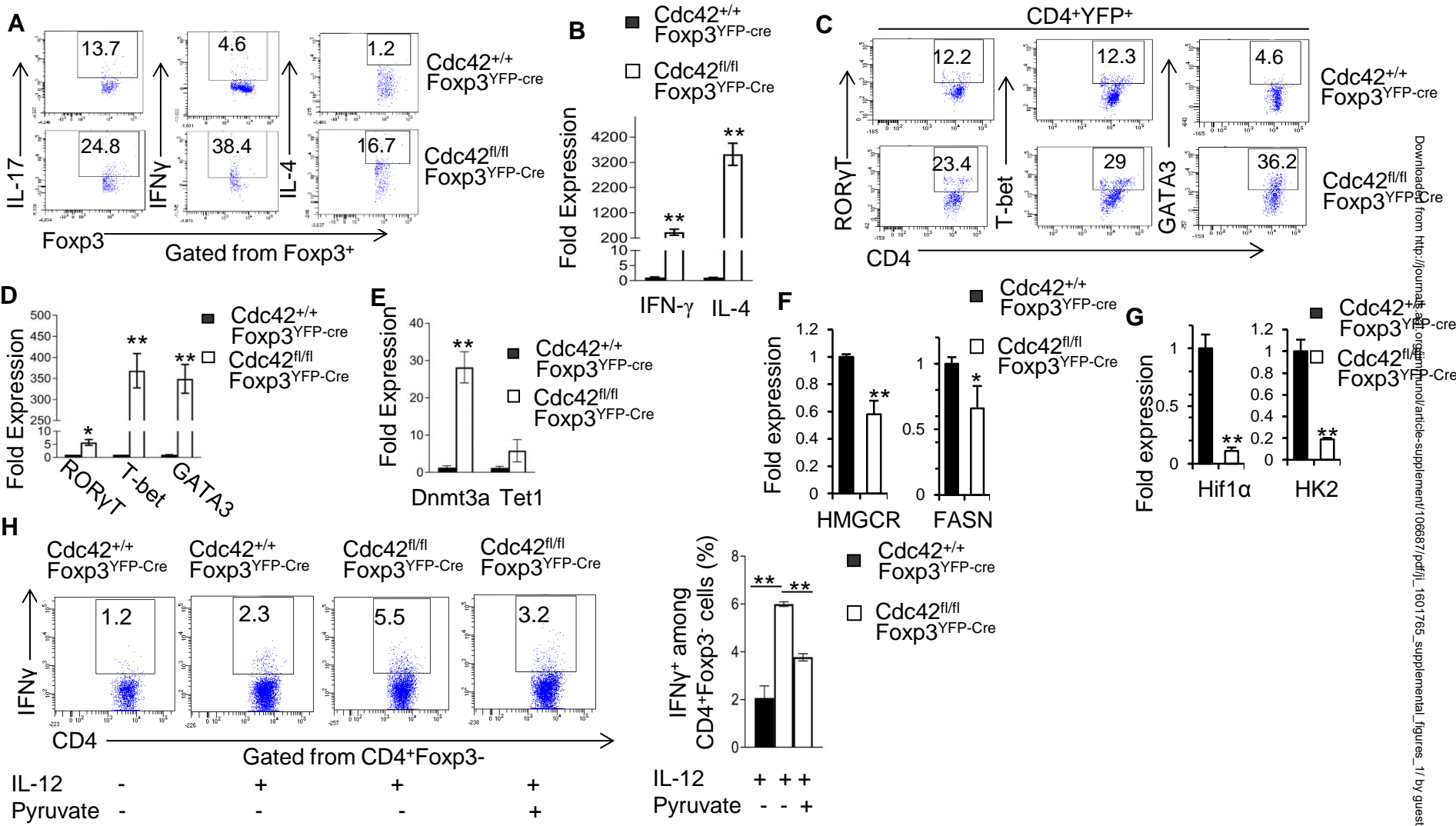
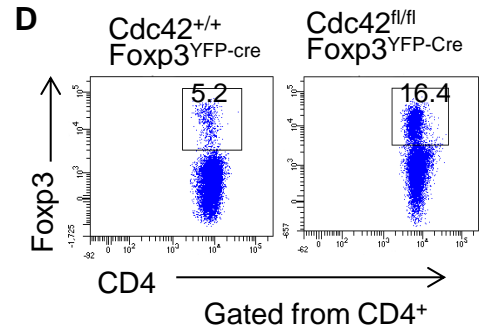
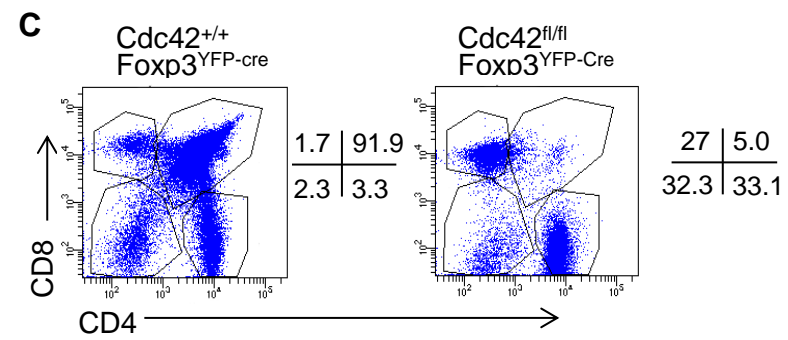
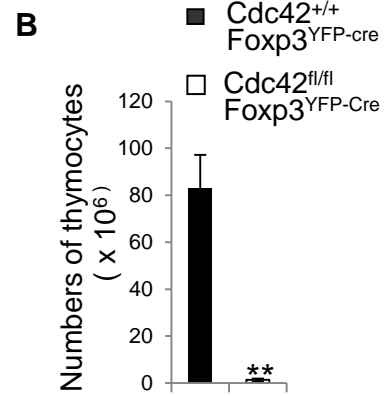
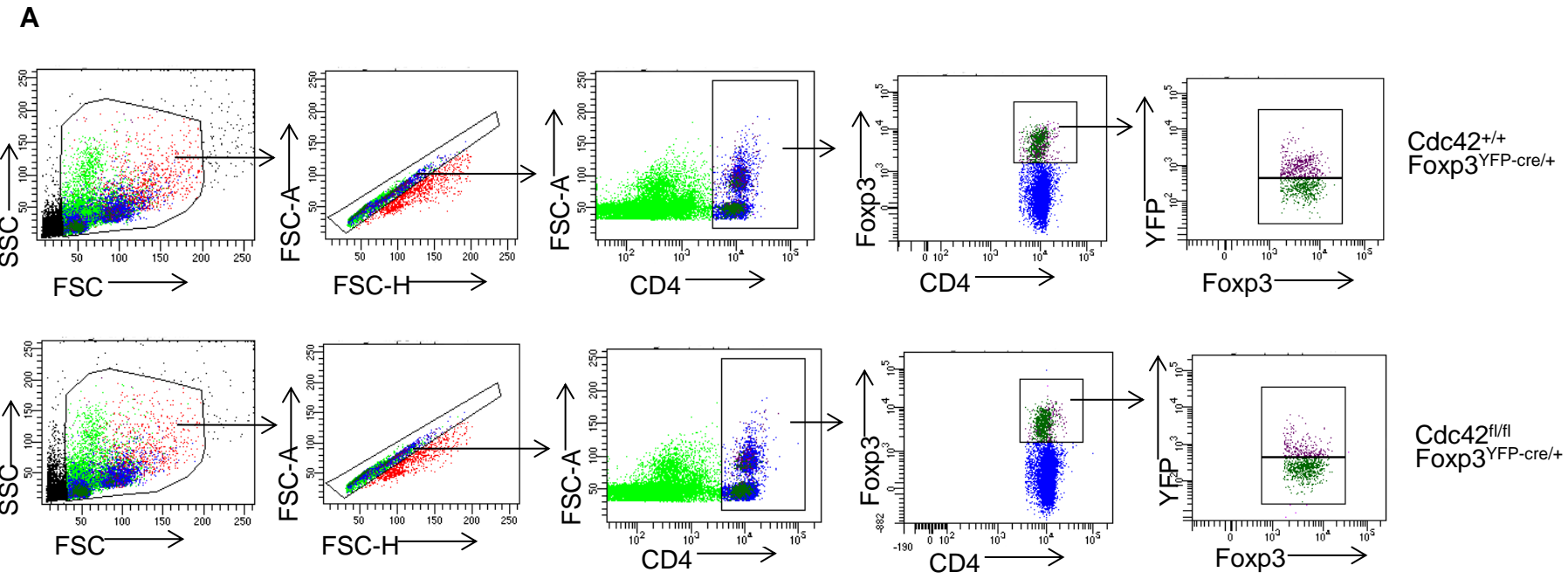


Supplemental Figure 2. (A) Flow-sorting strategy of nTreg cells from peripheral lymphoid organs of *Cdc42^{+/+}Foxp3^{YFP-Cre}* and *Cdc42^{fl/fl}Foxp3^{YFP-Cre}* mice. PE was used to exclude auto-fluorescent cells that showed on the diagonal axis in YFP vs PE dot blots. **(B)** Treg-specific deletion of *Cdc42* leads to an increased expression of transcriptional factors characteristic of Th1 and Th2 cells in non-Treg cells. Representative flow cytogram of RORγT, T-bet and GATA-3 staining in CD4⁺YFP⁻ cells from the spleen of *Cdc42^{+/+}Foxp3^{YFP-Cre}* and *Cdc42^{fl/fl}Foxp3^{YFP-Cre}* mice is shown. Numbers indicate percentages of RORγT⁺, T-bet⁺ and GATA3⁺ cells. **(C)** Treg-specific deletion of *Cdc42* leads to impaired Treg survival. Representative flow cytogram of Annexin V and 7-AAD staining in CD4⁺YFP⁺ cells from the spleen of *Cdc42^{+/+}Foxp3^{YFP-Cre}* and *Cdc42^{fl/fl}Foxp3^{YFP-Cre}* mice is shown. Numbers indicate percentages of cells in the corresponding quadrants. n = 5.



Supplemental Figure 3. (A-E) Treg-specific deletion of *Cdc42* leads to Treg instability. **(A)** Representative flow cytogram of staining of IL-17, IFN- γ and IL-4 among Foxp3⁺ cells from the spleen of *Cdc42*^{+/+}Foxp3^{YFP-cre} and *Cdc42*^{fl/fl}Foxp3^{YFP-cre} mice. **(B)** Real-time RT-PCR analysis of mRNA expression of IFN- γ and IL-4 in CD4⁺YFP⁺ cells from the spleen of *Cdc42*^{+/+}Foxp3^{YFP-cre} and *Cdc42*^{fl/fl}Foxp3^{YFP-cre} mice. **(C)** Representative flow cytogram of ROR γ T, T-bet and GATA-3 staining in CD4⁺YFP⁺ cells from the spleen of *Cdc42*^{+/+}Foxp3^{YFP-cre} and *Cdc42*^{fl/fl}Foxp3^{YFP-cre} mice. **(D)** Real-time RT-PCR analysis of mRNA expression of ROR γ T, T-bet and GATA-3 in CD4⁺YFP⁺ cells from the spleen of *Cdc42*^{+/+}Foxp3^{YFP-cre} and *Cdc42*^{fl/fl}Foxp3^{YFP-cre} mice. **(E)** Real-time RT-PCR analysis of mRNA expression of DNMT3A and TET1 in CD4⁺YFP⁺ cells from the spleen of *Cdc42*^{+/+}Foxp3^{YFP-cre} and *Cdc42*^{fl/fl}Foxp3^{YFP-cre} mice. **(F-H)** Treg-specific deletion of *Cdc42* downregulates lipid metabolism and glycolysis genes in nTreg cells and restoration of glycolysis rescues instability of *Cdc42*-deficient nTreg. **(F)** Real-time RT-PCR analysis of mRNA expression of lipid metabolism genes HMGCR and FASN in CD4⁺Foxp3⁺ cells from the spleen of *Cdc42*^{+/+}Foxp3^{YFP-cre} and *Cdc42*^{fl/fl}Foxp3^{YFP-cre} mice. **(G)** Real-time RT-PCR analysis of mRNA expression of glycolysis genes Hif1 α and HK2 in CD4⁺Foxp3⁺ cells from the spleen of *Cdc42*^{+/+}Foxp3^{YFP-cre} and *Cdc42*^{fl/fl}Foxp3^{YFP-cre} mice. **(H)** CD4⁺CD25⁺YFP⁺ nTreg cells purified from *Cdc42*^{+/+}Foxp3^{YFP-cre} and *Cdc42*^{fl/fl}Foxp3^{YFP-cre} mice were cultured for 36 h with or without anti-CD3/-CD28 and IL-12 (50 ng/ml), in the presence or absence of 2 mM pyruvate, and costained for CD4, Foxp3, and IFN- γ . Representative flow cytogram of IFN- γ staining among CD4⁺Foxp3⁺ cells is shown (left). Numbers in the dot plots indicate percentages of IFN- γ ⁺ cells. Average percentages of CD4⁺Foxp3⁺IFN- γ ⁺ cells are shown in bar graph (right). n = 5. Error bars indicate SD. *p < 0.05, **p < 0.01.



Supplemental Figure 4. (A) Gating strategy of Foxp3⁺YFP⁺ and Foxp3⁺YFP⁻ cells from the spleen of Cdc42^{+/+}Foxp3^{YFP-Cre/+} and Cdc42^{fl/fl}Foxp3^{YFP-Cre/+} mice. **(B)** Total thymocyte numbers in Cdc42^{+/+}Foxp3^{YFP-Cre} and Cdc42^{fl/fl}Foxp3^{YFP-Cre} mice. **(C)** Representative flow cytogram of thymocytes from Cdc42^{+/+}Foxp3^{YFP-Cre} and Cdc42^{fl/fl}Foxp3^{YFP-Cre} mice stained for CD4 and CD8. Numbers indicate percentages of CD4⁻CD8⁻, CD4⁺CD8⁺, CD4⁺ and CD8⁺ cells in corresponding quadrant. **(D)** Representative flow cytogram of Foxp3 staining (gated on CD4⁺ thymocytes) in thymocytes from Cdc42^{+/+}Foxp3^{YFP-Cre} and Cdc42^{fl/fl}Foxp3^{YFP-Cre} mice. Numbers indicate percentages of CD4⁺Foxp3⁺ cells. n = 5. Error bars indicate SD. **p < 0.01.